

# Time-resolved *in situ* X-ray diffraction in the crystallization of $\text{VOHPO}_4 \cdot 0.5\text{H}_2\text{O}$

L. O'Mahony<sup>a,b,\*</sup>, J. Henry<sup>a</sup>, D. Sutton<sup>a</sup>, T. Curtin<sup>a,b</sup>, and B.K. Hodnett<sup>a,b</sup>

<sup>a</sup>Materials and Surface Science Institute, University of Limerick, Limerick, Ireland

<sup>b</sup>Department of Chemical and Environmental Sciences, University of Limerick, Limerick, Ireland

Received 29 May 2003; accepted 5 August 2003

Time-resolved *in situ* X-ray diffraction was used to study the formation of the vanadium phosphorous oxide (VPO) catalytic precursor phase  $\text{VOHPO}_4 \cdot 0.5\text{H}_2\text{O}$  in organic media. *In situ* energy-dispersive X-ray diffraction has identified a new phase at early reaction times (less than 300 s) at *d*-spacings of 7.5 and 3.1 Å. At short reaction times, thin symmetrical platelets of 10 by 10 μm dimensions were observed. Scanning Electron Microscopy combined with energy-dispersive X-ray analysis (EDXA) indicated that these platelets contained vanadium and phosphorus. The features at 7.5 Å, which shift to 6.7 Å during the first 20 min of synthesis, are associated with  $\text{VOPO}_4 \cdot 2\text{H}_2\text{O}$  and  $\text{VOPO}_4 \cdot \text{H}_2\text{O}$  and disappear as  $\text{VOHPO}_4 \cdot 0.5\text{H}_2\text{O}$  forms. The platelets appeared to delaminate, possibly associated with the strain generated when a *d*-spacing shifts from 7.5 Å to 6.7 Å, from which epitaxial growth of the  $\text{VOHPO}_4 \cdot 0.5\text{H}_2\text{O}$  into the familiar rosette morphology occurs.

**KEY WORDS:** vanadyl hydrogen phosphate hemihydrate; *in situ* energy-dispersive X-ray diffraction; nucleation; crystallization.

## 1. Introduction

The principle phase present in vanadium phosphorus oxide catalysts used for *n*-butane transformation to maleic anhydride is  $(\text{VO})_2\text{P}_2\text{O}_7$ . This phase forms by the topotactic transformation of  $\text{VOHPO}_4 \cdot 0.5\text{H}_2\text{O}$  during heating in an *n*-butane air mixture close to the eventual reaction temperature [1–10]. In turn,  $\text{VOHPO}_4 \cdot 0.5\text{H}_2\text{O}$  is prepared by reducing  $\text{V}_2\text{O}_5$  at reflux in aqueous HCl or using an alcohol followed by addition of *ortho*- $\text{H}_3\text{PO}_4$  and continuing to reflux for 2–4 h [3].

The crystalline habit, particle size and P:V ratio of the eventual catalyst is very similar to the features in the precursor. Indeed, the preparation methods have been developed that optimize the exposure of the (200) basal plane in  $(\text{VO})_2\text{P}_2\text{O}_7$ . This plane is associated with the (001) basal plane of  $\text{VOHPO}_4 \cdot 0.5\text{H}_2\text{O}$  [11–16].

The synthesis route and reaction conditions during synthesis affect the morphology of  $\text{VOHPO}_4 \cdot 0.5\text{H}_2\text{O}$  and ultimately the catalyst performance [1–10]. The precursor proposed by the aqueous synthesis route is generally more crystalline than that prepared by the organic route [3,6]. The organic synthesis route with isobutanol results in a platelet morphology or a rosette morphology where individual platelets agglomerate. With *sec*-butyl alcohol or *t*-butyl alcohol, well-formed platelets form without agglomeration [7].

This communication describes *in situ* X-ray diffraction studies of the evolution of phases during the synthesis of  $\text{VOHPO}_4 \cdot 0.5\text{H}_2\text{O}$ , combined with an

*ex situ* microscopy study, which concentrates on samples retrieved from the synthesis mixture at very short reaction times (< 20 min).

## 2. Experimental

A series of VPO (vanadium phosphorous oxide) precursors were prepared by refluxing  $\text{V}_2\text{O}_5$  (Merck) in a 90:10 alcohol mixture of 2-methyl propan-1-ol (BDH Analar) and benzyl alcohol (Riedel-de Haen) for 4 h at 108 °C. An 85% orthophosphoric acid (Aldrich) solution was then added to the resulting vanadium oxide suspension and was refluxed for a further 2 h. The reactant P:V mole ratio was 1:1. Samples were recovered at various times throughout the reaction following phosphorous addition. The recovered solids were filtered and dried at 120 °C.

*Ex situ* X-ray diffraction was performed on a Philips X'pert PRO MPD instrument using the Cu K $\alpha$  line at 1.542 Å operated at 40 kV and a current of 35 mA.

A Focused Ion Beam microscope, FEI 200, was used to obtain precursor images. Samples were coated with gold in an Emitech K550 sputter coater. The beam energy is typically 30 keV, with a beam current in the range of 1–11500 pA. Energy-dispersive X-ray analysis was performed in a Joel-JSM 840 scanning electron microscope.

In preparation for *in situ* diffraction studies,  $\text{V}_2\text{O}_5$  (Merck) was refluxed in a 90:10 alcohol mixture of 2-methyl propan-1-ol (BDH Analar) and benzyl alcohol (Riedel-de Haen) for 4 h. *Ortho*- $\text{H}_3\text{PO}_4$  was added to these suspensions (P:V = 1:1) in a Teflon-lined stain-

\* To whom correspondence should be addressed.

less steel cell under constant stirring. The evolution of crystalline phases with time was then recorded *in situ* using the energy-dispersive X-ray diffraction setup at Station 16.4 of the UK Synchrotron Radiation Source (SRS) at the CLRC Daresbury Laboratory, UK (shown in figure 1) [17–19].

This system utilizes a multidetector system that collects XRD patterns from a sample simultaneously at different angles. Two detectors were used, which recorded X-ray diffraction patterns in the regions of 2–5 and 4–15 Å, respectively.

### 3. Results and discussion

Figure 2 presents the XRD patterns of the series of solids isolated from the vanadyl hydrogen phosphate hemihydrate precursor preparation at various times following addition of orthophosphoric acid (85%  $\text{H}_3\text{PO}_4$ ). At early reaction times, the main reflections of  $\text{V}_2\text{O}_5$  were observed. These reflections began to diminish within 10 min of reaction with the resultant formation of the characteristic hemihydrate reflections. One curious feature of these diffraction patterns is the observation of a reflection at 6.9 Å for the sample recovered after 2 min of synthesis. Apart from this feature, all the reflections in figure 2 are associated with  $\text{V}_2\text{O}_5$  or  $\text{VOHPO}_4 \cdot 0.5\text{H}_2\text{O}$ .

Figures 3 and 4 present the *in situ* diffraction patterns of the VPO phases that developed when phosphoric acid was added to  $\text{V}_2\text{O}_5$  in organic media. A reflection at 4.91 Å is observed in all patterns and is related to Teflon from the lining of the sample cell. Figure 3 presents the XRD patterns recorded at  $d$ -spacings 2–5 Å. These *in situ* diffraction patterns are consistent with the data observed in figure 2. At short reaction times, the reflections are primarily those of  $\text{V}_2\text{O}_5$ . With increasing reaction time, characteristic reflections of  $\text{V}_2\text{O}_5$  disappear and those of the hemihydrate precursor phase emerge. The (010), (101), and (310) reflections of  $\text{V}_2\text{O}_5$  decrease with time of reaction and completely disappear after 24–28 min. By this time, the (101), (121), and (220) reflections of  $\text{VOHPO}_4 \cdot 0.5\text{H}_2\text{O}$  begin to form. A consistent feature for all *in situ* diffraction patterns was the development of a reflection at 3.1 Å. This is not a feature of the XRD pattern of  $\text{V}_2\text{O}_5$ . The (201) reflection of  $\text{VOHPO}_4 \cdot 0.5\text{H}_2\text{O}$  occurs at 3.1 Å.

Figure 4 presents the patterns recorded *ex situ* at  $d$ -spacings 4–15 Å. The patterns show a reflection at 7.5 Å. This reflection evolves at an early stage in the reaction (2 min) and is observed to shift to 6.7 Å after 16 min. By this time, the (001) reflection of the hemihydrate precursor emerges at 5.7 Å with a maximum intensity after 50-min synthesis time.

Figure 5 presents microscopy (Focused Ion Beam) of the samples recovered at intervals throughout the

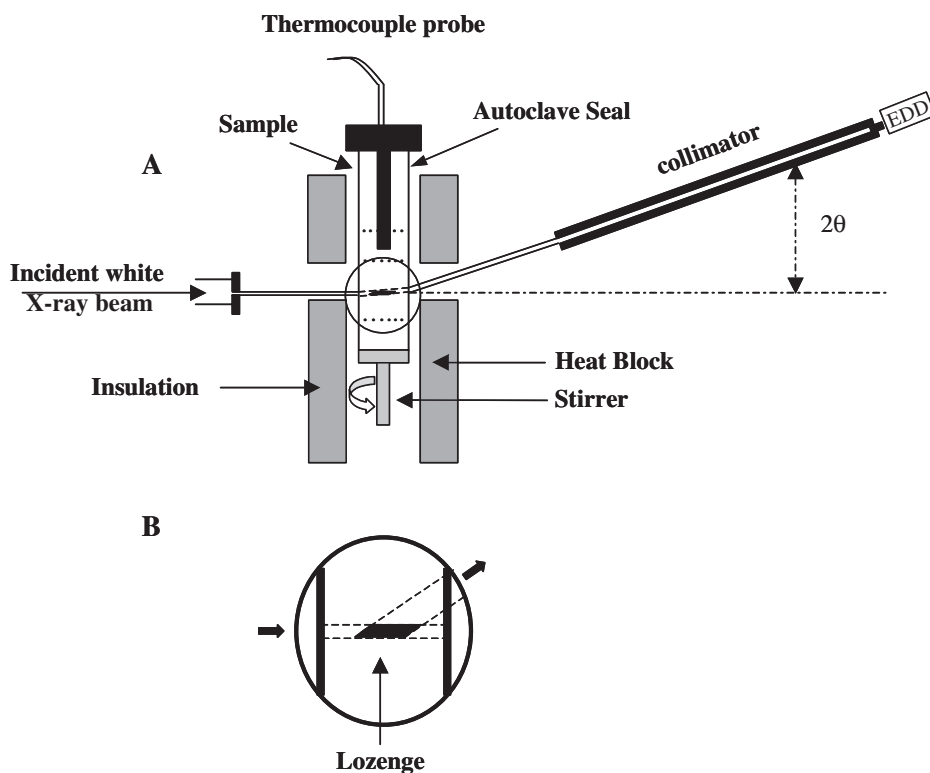


Figure 1. Schematic diagram of the experimental cell setup used to record the *in situ* energy-dispersive diffraction data on Station 16.4 at the SRS, Daresbury Laboratory, UK.

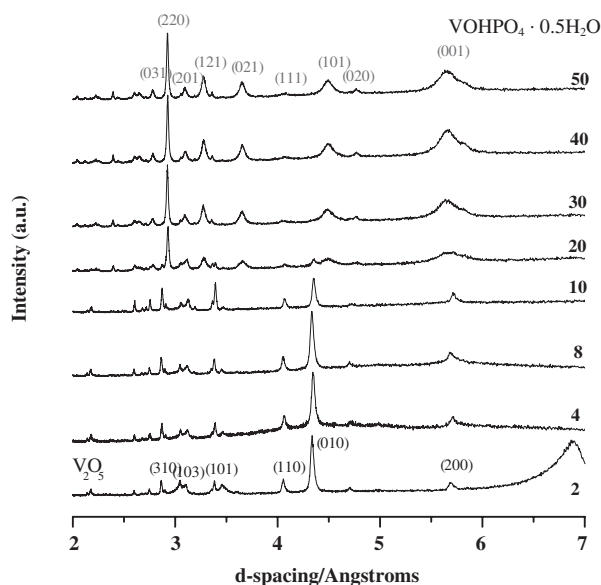


Figure 2. *Ex situ* X-ray diffraction presenting the evolution of  $\text{VOHPO}_4 \cdot 0.5\text{H}_2\text{O}$  during phosphorous interaction with  $\text{V}_2\text{O}_5$  in organic media. (P : V ratio = 1 : 1, reaction time in minutes.)

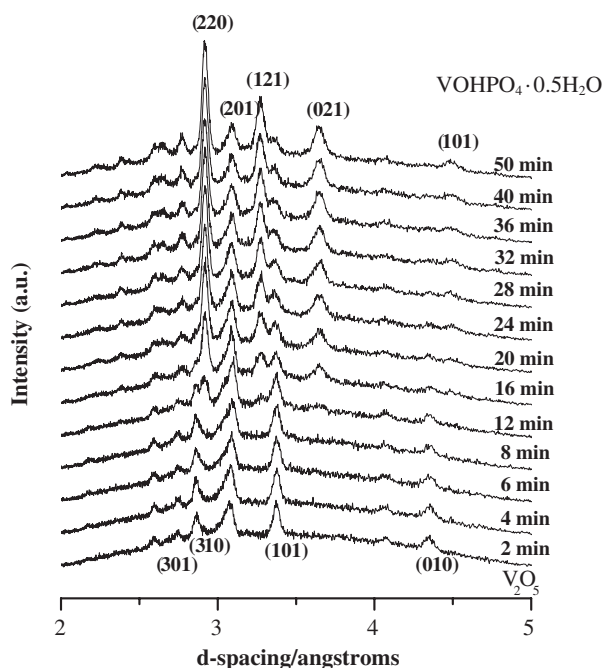


Figure 3. *In situ* energy-dispersive XRD patterns of  $\text{VOHPO}_4 \cdot 0.5\text{H}_2\text{O}$  evolution from  $\text{V}_2\text{O}_5$  at  $103^\circ\text{C}$  with a reactant P : V molar ratio of 1 : 1.

crystallization process. It can be readily observed from the imaging of samples harvested at short reaction times (2–8 min) (figures 5(a)–(c)) that thin platelet growth has occurred. In addition to undissolved  $\text{V}_2\text{O}_5$ , and the regular rosette like features normally associated with  $\text{VOHPO}_4 \cdot 0.5\text{H}_2\text{O}$  prepared in organic media, flat, square-shaped platelets  $10$  by  $10\ \mu\text{m}$  appear. In some

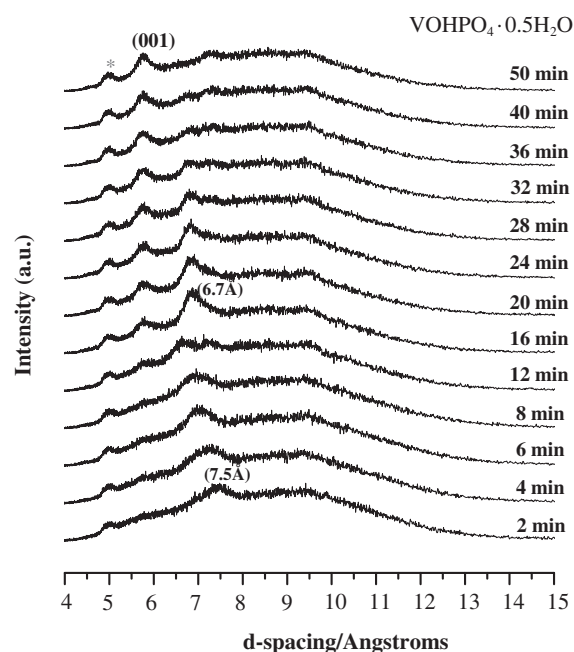


Figure 4. *In situ* energy-dispersive XRD patterns of  $\text{VOHPO}_4 \cdot 0.5\text{H}_2\text{O}$  evolution from  $\text{V}_2\text{O}_5$  at  $103^\circ\text{C}$  with a reactant P : V molar ratio of 1 : 1 (\*Reflection of Teflon liner at  $4.9\ \text{\AA}$ ).

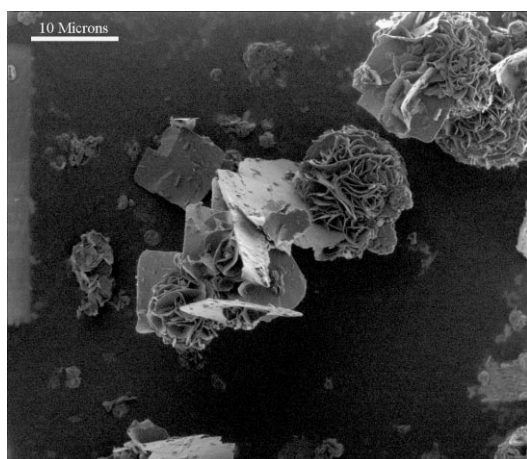
instances, these become distorted with rosette-shaped hemihydrate particles appearing to grow out from the basal plane of the platelets (see figures 5(a) and (b)). Small numbers of  $\text{V}_2\text{O}_5$  crystals are still evident even at 20 min of reaction. But by this time the majority of features observed by microscopy were folded and distorted platelets and poorly formed rosettes associated with the developing hemihydrate precursor.

In this work, we associate the reflections observed *in situ* at  $7.5$ – $6.7\ \text{\AA}$  and at  $3.1\ \text{\AA}$ , with the platelets observed by microscopy. The EDXA of these platelets indicated the presence of phosphorus in all cases. These platelets were never observed prior to the addition of phosphorus ( $o\text{-H}_3\text{PO}_4$ ). The reflections are consistent with the formation of  $\text{VOPO}_4 \cdot 2\text{H}_2\text{O}$  and  $\text{VOPO}_4 \cdot \text{H}_2\text{O}$  [20–23]. Another key feature of this work is the observation that there is some element of delamination of the platelets, possibly as a mechanism whereby strain is released as the  $d$ -spacing changes from  $7.5\ \text{\AA}$  for the (001) reflection of  $\text{VOPO}_4 \cdot 2\text{H}_2\text{O}$  initially to a value of ca.  $6.7\ \text{\AA}$  for the (001) reflection of  $\text{VOPO}_4 \cdot \text{H}_2\text{O}$  after a synthesis time of ca. 30 min. In some instances (figure 5), the platelets are observed to curl up at the edges, and in some cases, the uppermost layers crack at the platelet center and then point outward as they delaminate.

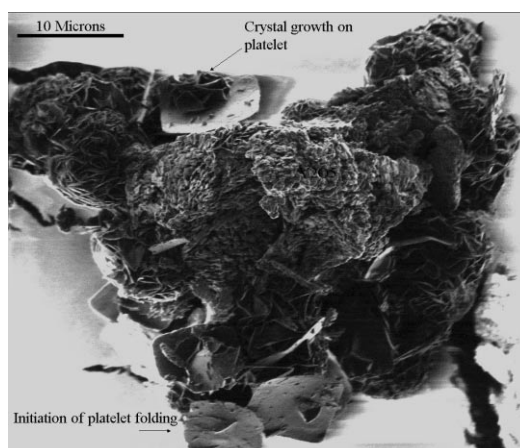
Here, we hypothesize that the reflections appearing at  $7.5$  and  $3.1\ \text{\AA}$  are associated with planes parallel to the basal plane of the platelets. As the  $d$ -spacing shrinks to  $6.7\ \text{\AA}$ , strain develops inside the platelets, resulting in delamination as a means of relieving strain. Delamina-

### Focused Ion Beam Imaging

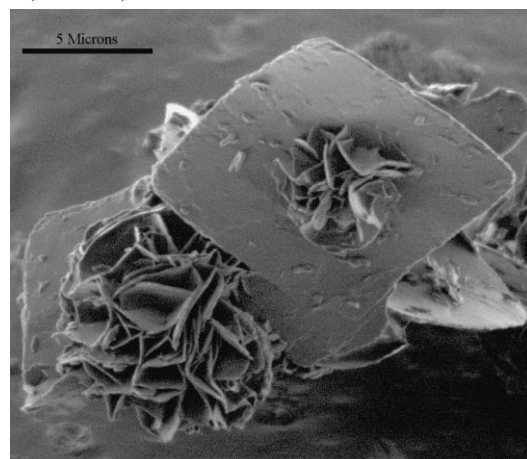
A (2 minutes)



C (8 minutes)



B (2 minutes)



D (20 minutes)

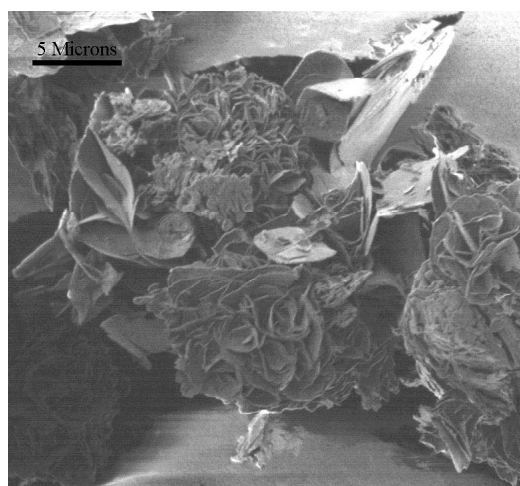


Figure 5. FIB images of samples recovered after (a) 2, (b) 2, (c) 8, and (d) 20 min of reaction following phosphorus addition.

tion exposes an increased number of edges with  $d$ -spacings of 6.7 and 3.1 Å, close in dimension to the (001) plane at 5.7 Å and the (201) plane at 3.1 Å, thus facilitating epitaxial growth of the hemihydrate from these attachment points. The edges of the delaminated platelets expose  $d$ -spacings at 6.7 and 3.1 Å. We hypothesize that these platelets grow into the (001) (at 5.7 Å) and (201) (at 3.1 Å) planes of  $\text{VOHPO}_4 \cdot 0.5\text{H}_2\text{O}$ .

Figure 6 presents a schematic of the interface between the two materials. According to the scheme, the (201) plane of the hemihydrate grows on to 3.1 Å plane of the platelet, and this feature is important in facilitating the epitaxial growth of the hemihydrate from the platelets. The eventual rosette like habit of  $\text{VOHPO}_4 \cdot 0.5\text{H}_2\text{O}$  then emerges from the delamination of these intermediate platelet structures.

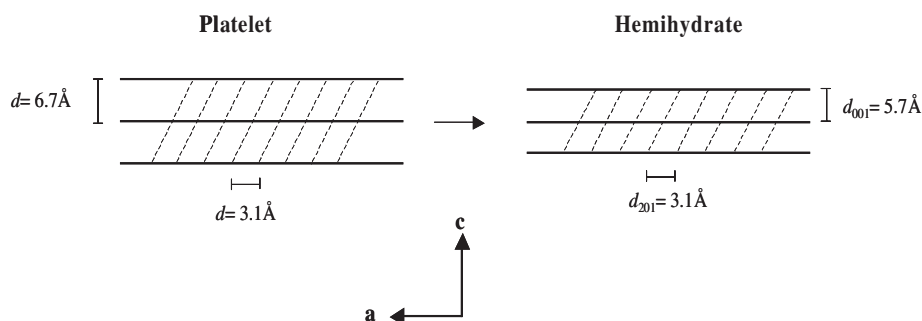


Figure 6. Schematic of crystallographic planes in (a) platelets and (b)  $\text{VOHPO}_4 \cdot 0.5\text{H}_2\text{O}$  viewed along the b [010] direction.



#### 4. Conclusion

*In situ* X-ray diffraction allowed the detection of  $\text{VOPO}_4 \cdot 2\text{H}_2\text{O}$  and  $\text{VOPO}_4 \cdot \text{H}_2\text{O}$  as precursors in the synthesis of  $\text{VOHPO}_4 \cdot 0.5\text{H}_2\text{O}$ . Subsequent microscopy indicated that the  $\text{V}^{5+}$  hydrates exhibit platelet-type habits and forms the nucleation point from which  $\text{VOHPO}_4 \cdot 0.5\text{H}_2\text{O}$  grows.

#### Acknowledgments

The authors acknowledge financial support from the Materials and Surface Science Institute, University of Limerick, Limerick, Ireland. Leonard O'Mahony would like to thank the CLRC Daresbury Laboratory, UK, for beam time on Station 16.4 and Dr. David Talyor for his assistance with setting up the synthesis cell.

#### References

- [1] M. Abon and J.C. Volta, Appl. Catal., A: Gen. (1997) 157.
- [2] G. Centi, Catal. Today 16 (1993) 173.
- [3] G. Centi, F. Trifiro, J.R. Ebner and V.M. Franchetti, Chem. Rev. 88 (1988) 55.
- [4] B.K. Hodnett, Catal. Rev. Sci. Eng. 27 (1985) 373.
- [5] B.K. Hodnett, *Heterogeneous Catalytic Oxidation: Fundamentals and Technological Aspects of the Selective and Total Oxidation of Organic Compounds* (Wiley, New York, 2000).
- [6] F. Cavani and F. Trifiro, Catalysis 11 (1994) 246.
- [7] H.S. Horowitz, C.M. Blackstone, A.W. Sleight and G. Teufer, Appl. Catal. 38 (1988) 193.
- [8] G.J. Hutchings, Appl. Catal. 72 (1991) 1.
- [9] C.J. Kiely, A. Burrows, S. Sajip, G.J. Hutchings, M.T. Sananes, A. Tuel and J.C. Volta, J. Catal. 162 (1996) 31.
- [10] G.J. Hutchings, M.T. Sananes, S. Sajip, C.J. Kiely, A. Burrows, I.J. Ellison and J.C. Volta, Catal. Today 33 (1997) 161.
- [11] M. Abon, K.E. Bere, A. Tuel and P. Delichere, J. Catal. 156 (1995) 28.
- [12] J.R. Ebner and M.R. Thompson, Catal. Today 16 (1993) 51.
- [13] G.J. Hutchings, A. Desmartin-Chomel, R. Olier and J.C. Volta, Nature 368 (1994) 41.
- [14] G.J. Hutchings, C.J. Kiely, M.T. Sananes-Schulz, A. Burrows and J.C. Volta, Catal. Today 40 (1998) 273.
- [15] G.J. Hutchings, A. Burrows, S. Sajip, C.J. Kiely, K.E. Bere, J.C. Volta, A. Tuel and M. Abon, in *3rd World Congress on Oxidation Catalysis* (1997) 210.
- [16] V.V. Gulians, S.A. Holmes, J.B. Benziger, P. Heaney, D. Yates and I.E. Wachs, J. Mol. Catal. A: Chem. 172 (2001) 265.
- [17] P. Barnes, A.C. Jupe, S.L. Colston, S.D. Jacques, A. Grant, T. Rathbone, M. Miller, S.M. Clark and R.J. Cernik. Nucl. Instrum. Methods Phys. Res., Sect. B 134 (1998) 310.
- [18] S.M. Clark, R.J. Cernick, A. Grant, S. York, P.A. Atkinson, A. Gallagher, D.G. Stokes, S.R. Gregory, N. Harris, W. Smith, M. Hancock, M.C. Miller, K. Ackroyd, R. Farrow and R. Frances. Mater. Sci. Forum 228–231 (1996) 213.
- [19] S.M. Clark, Nucl. Instrum. Methods Phys Res., Sect. A 381 (1996) 161.
- [20] E. Kestemann, M. Merzouki, B. Taouk, E. Bordes and R. Contractor, *Preparation of Catalysts VI, Studies in Surface Science and Catalysis Series*, Vol. 91, G. Poncelet et al. (eds), (1995) p. 707.
- [21] E. Bordes and P. Courtine, C. R. Acad. Sci. Paris 274C (1972) 1375.
- [22] E. Bordes and P. Courtine, Ann. Chim. Paris, 8 (1973) 105.
- [23] E. Bordes, P. Courtine and J.W. Johnson, J. Solid State Chem. 55 (1984) 270.